

Published in final edited form as:

*J Neuroendocrinol.* 2011 January ; 23(1): 52–64. doi:10.1111/j.1365-2826.2010.02076.x.

## Characterisation of Arcuate Nucleus Kisspeptin/Neurokinin B Neuronal Projections and Regulation during Lactation in the Rat

Cadence True<sup>\*</sup>, Melissa Kirigiti<sup>\*</sup>, Philippe Ciofi<sup>†,‡</sup>, Kevin L. Grove<sup>\*</sup>, and M. Susan Smith<sup>\*</sup>

<sup>\*</sup> Division of Neuroscience, Oregon National Primate Research Center, Oregon Health & Science University, Beaverton, Oregon, 97006

<sup>†</sup> Neurocentre Magendie-U862 INSERM

<sup>‡</sup> Université de Bordeaux 2, F-33077 Bordeaux, France

### Abstract

Lactation results in negative energy balance in the rat leading to decreased gonadotrophin-releasing hormone (GnRH) release and anoestrus. Inhibited GnRH release may be a result of decreased stimulatory tone from neuropeptides critical for GnRH neuronal activity, such as kisspeptin (Kiss1) and neurokinin B (NKB). The present study aimed to identify neuronal projections from the colocalised population of Kiss1/NKB cells in the arcuate nucleus (ARH) using double-label immunohistochemistry to determine where this population may directly regulate GnRH neuronal activity. Additionally, the present study further examined lactation-induced changes in the Kiss1 system that could play a role in decreased GnRH release. The colocalised ARH Kiss1/NKB fibres projected primarily to the internal zone of the median eminence (ME) where they were in close proximity to GnRH fibres; however, few Kiss1/NKB fibres from the ARH were seen at the level of GnRH neurones in the preoptic area (POA). Arcuate Kiss1/NKB peptide levels were decreased during lactation consistent with previous mRNA data. Surprisingly, anteroventral periventricular (AVPV) Kiss1 peptide levels were increased, whereas *Kiss1* mRNA levels were decreased during lactation, suggesting active inhibition of peptide release. These findings indicate ARH Kiss1/NKB and AVPV Kiss1 appear to be inhibited during lactation, which may contribute to decreased GnRH release and subsequent reproductive dysfunction. Furthermore, the absence of a strong ARH Kiss1/NKB projection to the POA suggests regulation of GnRH by this population occurs primarily at the ME level via local projections.

### Keywords

Arcuate nucleus; lactation; kisspeptin; neurokinin B

---

Gonadotrophin-releasing hormone (GnRH) is a critical component of the hypothalamic-pituitary-gonadal (HPG) axis governing regulation of the gonadotrophins, luteinising hormone (LH) and follicle-stimulating hormone (FSH). When metabolic homeostasis is disrupted towards negative energy balance, the HPG axis is inhibited in female mammals, resulting in anovulation. This inhibition of cyclic reproductive function is largely attributed to decreases in GnRH release, although the upstream regulatory events leading to this decrease are not well understood.

---

© 2010 The Authors.

Correspondence to: M. Susan Smith, Oregon Health & Science University, Beaverton, 505 NW 185th Avenue, OR 97006, USA (smithsu@ohsu.edu).

Recent research into the regulation of GnRH release has focused largely on the powerful secretagogue kisspeptin (Kiss1) (1–4). Originally, a mutation in the human gene for the Kiss1 receptor GPR54 was found to result in hypogonadotropic hypogonadism, a disorder characterised by low GnRH release during development (5, 6). Subsequent research has demonstrated that Kiss1 administration alone causes large increases in circulating LH and FSH levels through a GnRH dependent mechanism (7–9). Importantly, rodent data have demonstrated that Kiss1 appears important for steroid feedback regulation of GnRH because the anteroventral periventricular (AVPV) Kiss1 population is linked to positive feedback and the arcuate nucleus (ARH) population is linked to negative feedback (10, 11). A recent study demonstrated that, similar to GPR54 mutations, human mutations in the neurokinin B (NKB) receptor, NK3, as well as NKB itself, resulted in hypogonadotropic hypogonadism, indicating that NKB may be another critical stimulator of GnRH release (12). NKB has also long been known to be inhibited by oestradiol and thus NKB may also contribute to negative steroid feedback of GnRH activity (13, 14). Interestingly, the Kiss1 population in the ARH is colocalised with NKB in the nonhuman primate (15), ewe (16), mouse (17) and the rat (present study).

A negative energy balance-induced GnRH inhibition may result from decreased stimulatory tone set by neuropeptides such as Kiss1 and NKB. Lactation in the rat is a well-studied model of negative energy balance, in which the high metabolic cost of milk production results in decreased GnRH release. Recent data have demonstrated a decrease in ARH *Kiss1* mRNA and Kiss1 peptide levels during lactation in the rat, as well as decreased NKB mRNA levels, although NKB peptide levels are unknown (18, 19). The Kiss1 population in the AVPV has also been linked to stimulating GnRH release, particularly in high oestrogen conditions during pro-oestrus leading to the LH surge, suggesting inhibition of this population could also contribute to decreased stimulatory tone for GnRH release (2, 4, 20, 21).

Although ARH Kiss1/NKB neurones have previously been linked to GnRH regulation, the site of regulatory contact between these two neuronal populations is not well understood. The presence of GPR54 mRNA in GnRH cell bodies and NK3 on GnRH fibres suggests direct regulation of GnRH by NKB and Kiss1 (22–24). Additional evidence for direct regulation is the presence of both Kiss1-immunoreactive (–ir) fibres as well as NKB-ir fibres in the median eminence (ME), near GnRH fibres, and in the preoptic area (POA), near GnRH cell bodies (15, 23, 25, 26). Therefore, both Kiss1 and NKB may regulate GnRH release at fibres in the ME, as well as cell bodies in the POA, although the nuclei from which these Kiss1 and NKB fibres originate remains unclear.

The regulation of Kiss1 and NKB populations as well as their possible projections to GnRH cells could prove to be critical for our understanding of GnRH inhibition during negative energy balance. The present study aimed: (i) to use double-label immunohistochemistry to characterise projections of ARH Kiss1/NKB fibres and (ii) to determine lactation-induced changes in these neuropeptides, which may contribute to decreased GnRH release.

## Materials and methods

### Animals

Adult female Wistar rats (200–220 g; Simonsen) were used in all studies. Animals were maintained under a 12 : 12 h light/dark cycle (lights on 07.00 h) throughout the experiment and allowed food (Purina Lab Chow 5001; Ralston-Purina, St Louis, MO, USA) and water *ad lib*. All protocols were approved by the Oregon National Primate Research Center Animal Care and Use Committee and conducted in accordance with NIH Guidelines for care and use of laboratory animals.

## Experiment 1: ME projections of ARH Kiss1/NKB neurones

Transgenic rats with green fluorescent protein (GFP) expression under the control of the GnRH promoter were used for immunohistochemistry to investigate ARH Kiss1/NKB projections to the ME, where GnRH fibres terminate. Ovariectomy was performed on all animals to remove negative steroid feedback and maximise ARH Kiss1 and NKB peptide expression. Adult ovariectomised (OVX) virgins animals ( $n = 4$ ) served as controls for comparison with adult lactating animals ( $n = 4$ ), which were OVX on day 2 of lactation. Animals were euthanised 8 days following OVX, which corresponded to day 10 of lactation. Day 10 of lactation is mid-lactation, a time when animals are known to be experiencing suppression of GnRH/LH and severe negative energy balance (18). Animals were anaesthetised under pentobarbital anesthesia and then perfused transcardially with ice cold saline followed by ice cold 4% paraformaldehyde in  $\text{NaPO}_4$  buffer (pH 7.4). Brains were removed and saturated for 24 h in paraformaldehyde followed by 24 h in 25% sucrose and then frozen on dry ice and stored at  $-80^\circ\text{C}$ . Fixed brain tissue was sectioned coronally at  $25\ \mu\text{m}$ , and collected serially into six groups, so that consecutive sections for a given series are approximately  $150\ \mu\text{m}$  apart. Tissue was cut using a sliding microtome and preserved in ethylene glycol cryoprotectant at  $-20^\circ\text{C}$ .

**Immunohistochemistry**—A single series of fixed tissue from each animal was used for immunohistochemistry experiments starting with a potassium phosphate buffer rinse followed by blocking in 2% donkey serum and 0.4% Triton X-100 for 30 min. Tissue was then incubated for 1 h at room temperature followed by 48 h at  $4^\circ\text{C}$  in a primary antibody solution. All antibodies were titrated to give an optimal signal and minimal background. The Millipore rabbit anti-Kiss1 antibody (Cat. #AB9754, Lot #LV1541898; Millipore, Billerica, MA, USA) used in the present study was initially characterised and distributed by Dr Alan Caraty (27). For immunohistochemistry, the Kiss1 antibody was used at a dilution of 1 : 1500 with fluorescence secondary detection. Pre-adsorption with  $10\ \mu\text{M}$  RFRP1 diminished labelling with this Kiss1 antibody, suggesting some cross-reaction. However, the lack of immunolabelled cells in the dorsomedial nucleus of the hypothalamus (DMH) where RFRP1 cells are located suggests that this cross-reactivity is minimal. Pre-adsorption with  $10\ \mu\text{M}$  Kiss1 abolished all staining. The guinea pig anti-NKB antibody (IS-3/61) has been fully characterised as specific for NKB (26, 28). This antibody was used at a dilution of 1 : 4000 for fluorescence labelling and 1 : 8000 for nickel-intensified 3,3'-diaminobenzidine tetrahydrochloride (NiDAB) labelling.

Following primary incubation, tissue was rinsed again before 1 h of incubation at room temperature in the secondary antibody cocktail. For fluorescence detection of the Kiss1 antibody, a 1 : 200 dilution of anti-rabbit Cy-5 (Jackson Immunoresearch, 711-175-152; Jackson Immunoresearch Laboratories, Inc., Bar Harbor, ME, USA) was used, whereas a 1 : 200 dilution of anti-guinea pig TRITC (Jackson Immunoresearch, 706-026-148; Jackson Immunoresearch Laboratories, Inc.) was used for detection of the NKB antibody. After secondary labelling, all tissue was immediately rinsed and mounted onto subbed slides and coverslipped for analysis by fluorescence microscopy. For NiDAB secondary labelling of the NKB antibody, tissue was again initially rinsed in buffer then incubated for 1 h at room temperature in a biotinylated donkey anti-guinea pig antibody (Jackson Immunoresearch; 706-066-148), followed by 1 h of incubation in A/B solution (1 : 222 dilution of both the A and B solution, Vectostain Elite ABC Kit; Vector Laboratories, Burlingame, CA, USA). Tissue was then incubated in a nickel sulphate DAB solution in sodium acetate until adequate staining was obtained. Mounted tissue was then dried on slides overnight and then dehydrated through increasing ethanol washes followed by two 5-min xylene washes and immediately coverslipped with Permount.

**Confocal microscopy and photomicrograph adjustments**—The triple-label immunofluorescence was imaged on a Leica TCS SP Confocal microscope (Leica Microsystems, Inc., Bannockburn, IL, USA). The  $\times 25$  images of GnRH-GFP (using a 488 nm AR laser), Kiss1-ir (using a 633 nm HeNe laser) and NKB-ir (using a 651 nm DPSS laser) were taken at 0.5  $\mu\text{m}$  increments along the z-axis of the tissue. Each wavelength was imaged sequentially to avoid bleed-through of different fluorophores to the opposing detector. Image stacks were then compiled using Metamorph software (Molecular Devices, Sunnyvale, CA, USA). Metamorph was also used to pseudocolour photomicrographs: Millipore Kiss1-ir was converted from infrared to green, and GnRH-GFP was converted from green to blue.

Further colour adjustments were carried out with Adobe Photoshop (Adobe Systems Inc., San Jose, CA, USA) to more accurately represent microscope displays. All confocal images were adjusted to 3.5  $\times$  3.5 inch image size and the resolution was adjusted to 150. Photomicrographs were lightly brightened by adjusting input levels to 25, 1.0 and 225. Pseudocolouring was performed using the ‘selective color replacement’ function to convert NKB staining from red to magenta, magenta staining (overlap of blue GnRH and red NKB labelling) to white, and to lighten blue GnRH fibres for better visibility.

**Fibre quantification and colocalisation analysis**—To determine the extent of Kiss1/NKB cell body colocalisation in the ARH, two ARH sections were used per animal. Cells were manually counted on one side of the ARH for both sections, then the percentage of colocalised cells was averaged across the two sections for each animal.

Single Kiss1 and NKB fibre content in the ME was examined from ME photomicrograph stacks using ImageJ software (National Institutes of Health Bethesda, MD, USA). Photomicrographs of two ME sections were used per animal and for all measurements, the values between the two ME were averaged per animal. The ME was traced, with tracing beginning at one corner of the ME and encompassing as much of the ME as was included in the photomicrograph, usually approximately one-half. The ‘Analyse Particles’ measurement was used, excluding particles that were composed of only two pixels or less, to determine the area of the region of interest that contains either Kiss1 or NKB staining. Particles were summed through the entire 28 planes (0.5  $\mu\text{m}$  thickness) and then normalised to the total area of the traced portion of the ME, and are expressed as particles/area examined. This analysis was performed for both Kiss1 and NKB labelling to determine whether lactation resulted in decreases in the total area of either Kiss1 or NKB total staining. In addition, Just Another Colocalization Program (JACoP) by S. Bolte and F. P. Cordelières (29) was used to calculate the Manders’ coefficients, which are the percentages of one staining that has the same location as another staining, aiming to determine the fraction of overlap between Kiss1 and NKB staining in the ME.

## Experiment 2: Rostral projections of ARH Kiss1/NKB neurones

To determine rostral projections of ARH Kiss1/NKB neurones, specifically in relation to GnRH cell bodies, a series of tissue sections were used from the animals described in Experiment 1, with one lactating animal excluded because of a technical error. Immunohistochemistry and confocal microscopy was performed as described above, except no NiDAB secondary labelling was used. For analysis of double-labelled fibre content at the level of GnRH neurones, two confocal images/animal were taken at the level of GnRH neurones for lactating ( $n = 3$ ) and control animals ( $n = 4$ ). No significant differences were observed in colocalised fibre content between the two groups, so they were combined for analysis. For each animal, one image was taken at the level of the medial septal nucleus, whereas another image was taken at the level of the nucleus of the diagonal band of Broca

(NDB). Images containing 28 stacks of 0.5  $\mu\text{m}$  thickness were once again analysed using the ImageJ plugin Just Another Colocalization Program (JACoP) by S. Bolte and F. P. Cordelières (29) aiming to determine the fraction of overlap between Kiss1 and NKB staining in the POA.

These two images per animal were also used to analyse close appositions on GnRH cells. Ten neurones across the two images were chosen at random and were analysed for close appositions of either Kiss1 or Kiss1/NKB staining. Close appositions were defined as any double-label with GnRH that was observed within a 1  $\mu\text{m}$  plane. Quantification was carried out similarly as described for the ME, although only the entire photomicrograph was analysed for the POA instead of using a region of interest, as was the case for the ME.

**Computer-assisted line drawing**—To generate the computer-assisted line drawing of Kiss1 and NKB fibre projections using confocal microscopy, one representative OVX virgin control case was selected and imaged at 10X, taking images at 1  $\mu\text{m}$  increments, from the NDB to the level of the ARH. For each section chosen, two adjacent images were taken along one side of the third ventricle. Forebrain levels were identified using the atlas Brain Maps: Structure of the Rat Brain (30). Montages of the confocal images were constructed using Adobe Illustrator (Adobe Systems Inc.). Lines colour-coded to represent either Kiss1-ir, NKB-ir, or double Kiss1/NKB-ir were drawn over contiguous fibre projections and terminal axonal fields using the pencil tool. At the level of the NDB, GnRH neurones were also traced using the pencil tool and later replaced with triangle symbols.

### Experiment 3: Regulation of Kiss1 and NKB populations during lactation

All comparisons between lactating and control conditions were performed in intact animals. Rats in the lactation group were received 17–18 days pregnant and the day of pup birth was defined as day 0 post-partum. On day 2/3, litters were adjusted to eight pups and tissue was collected day 10/11 post-partum. Tissue was collected from control animals on dioestrus after two consecutive 4–5-day oestrous cycles were observed by vaginal cytology. Immunohistochemistry was performed as described above using the Millipore rabbit Kiss1 antibody (dilution 1 : 1000) and the guinea pig NKB antibody (dilution 1 : 4000) and NiDAB secondary labelling.

**Cell counts**—For the ARH, cell counts for the total number of Kiss1-ir cells from both sides of the ventricle were summed together for four sections per animal ( $n = 4$  animals for lactating and dioestrous groups). The same protocol was carried out to determine ARH NKB-ir cell counts ( $n = 4$  animals for lactating group and  $n = 3$  animals for the dioestrous group). AVPV Kiss1-ir cell counts were performed in a similar manner, except that only three sections were counted per animal because of the small size of this nucleus ( $n = 3$  animals for lactation group and  $n = 4$  animals for the dioestrous group).

**In situ hybridisation**—Intact virgin and lactating groups were also used for *in situ* hybridisation. Animals were sedated with isoflurane before decapitation and rapid removal of the brain, which was subsequently frozen on powdered dry ice and stored at  $-80\text{ }^{\circ}\text{C}$  until sectioning. Fresh frozen brains were cut into a one-in-three series of 20  $\mu\text{m}$  coronal sections by cryostat (MICROM HM5000M; Carl Zeiss IMT Corporation, Maple Grove, MN, USA) from the AVPV through the bed nucleus of the stria terminalis (BST). *In situ* hybridisation was performed as described previously (18). One series of fresh frozen tissue per animal was briefly fixed in a phosphate-buffered paraformaldehyde solution and subsequently treated with 0.25% acetic anhydride in 0.1 M triethanolamine. Tissue was then taken through two washes in sodium saline citrate and dehydrated in a series of ethanol solutions, so that

delipidation in a chloroform wash could be performed. Tissue was then rehydrated through a reverse series of ethanol solutions and air-dried.

The *Kiss1* probe (a gift from the laboratory of Dr Robert Steiner, University of Washington), which has been characterised previously (31), was transcribed using a T7 polymerase in the presence of  $^{33}\text{P}$ . The radioactively-labelled probe was heat shocked and then diluted in hybridisation buffer (50% formamide, 6.25% dextran sulphate, 0.7% Ficoll, and 0.7% polyvinylpyrrolidone) and counted for final radioactive concentration. Slides were incubated in this diluted radioactive probe overnight in humidified chambers at 55 °C. After incubation, slides were washed in 4× SSC, ribonuclease A at 37 °C and in 0.1× SSC at 60 °C. Slides were then taken through a series of alcohols for dehydration.

For quantification of mRNA levels, *in situ* hybridisation slides were dipped in Kodak NTB emulsion (Eastman Kodak, Rochester, NY, USA) diluted in 600 mM ammonium acetate (Fisher Scientific Co., Pittsburgh, PA, USA) and placed in light-tight boxes containing desiccant at 4 °C. Slides were left to develop for 9 days. After development, slides were dehydrated in an alcohol series followed by washes in xylene and coverslipping with Permount.

Images of silver grains were taken under dark-field illumination using a CoolSNAP CCD camera (Photometrics, Tucson, AZ, USA) and analysed using the MetaMorph Imaging system (Universal Imaging Corp., West Chester, PA, USA). Silver grains were analysed using a size-constant sampling box that encompassed the entire AVPV and measured the integrated intensity. The same sampling box was used for background measurements by taking the integrated intensity in a region just adjacent to AVPV where no *Kiss1* mRNA is present. Background measurements were subtracted from the AVPV measurement to control for variations in emulsion levels. Comparisons of adjusted integrated intensities were compared between lactating and control animals for three sections per animal.

**Statistical analysis**—Student's t-test was used to compare lactation and dioestrous groups for *in situ* hybridisation data and cell counts. Data are represented as the mean  $\pm$  SEM.

## Results

### Experiment 1: ME projections of ARH Kiss1/NKB neurones

Immunohistochemistry confirmed previous findings of almost complete colocalisation of Kiss1-ir and NKB-ir cell bodies within the ARH, with  $97\% \pm 2.6$  of Kiss1 cells expressing NKB (Fig. 1). Because the ARH is the only known major site of Kiss1 and NKB colocalisation, detection of double-labelled fibres by immunohistochemistry can be used to differentiate Kiss1 projections specific to the ARH population.

ARH neurones are known to send projections to the ME where GnRH fibres terminate, and previous work has demonstrated the presence of both Kiss1 and NKB fibres in the ME (26, 31, 32). To determine whether Kiss1 and NKB fibres in the ME originate in the ARH, double-label immunohistochemistry was performed with fluorescent detection. Extensive Kiss1/NKB-ir fibres were seen in the ME primarily within the sub-ependymal and internal zones near GnRH fibres (Fig. 2). Single-labelled Kiss1- and NKB-ir fibres were also observed in the ME, and colocalisation analysis demonstrated that, in control animals, only  $39\% \pm 6$  of Kiss1 staining overlapped with NKB staining, and  $43\% \pm 4.3$  of NKB staining overlapped with Kiss1 staining in the ME. Therefore, although double-labelled Kiss1/NKB-ir fibres were common in the ME, they did not represent the majority of either Kiss1 or NKB fibre staining. Consistent with a previous study, single-labelled NKB-ir fibres were

detected in both the internal and external zone of the ME, (Fig. 2C,G) (33), whereas single-labelled Kiss1-ir fibres were found predominantly in the internal zone (32) (Fig. 2C,G), although occasionally fibres were seen in the external zone as well.

ME fibre distribution was analysed in both control and lactating animals to determine whether the lactating state resulted in changes in the possible regulation of GnRH by Kiss1/NKB fibres in the ME. No significant differences were observed between total Kiss1 fibres in control ( $6.41 \pm 1.31$  Kiss1-ir pixels/area) and lactating animals ( $6.27 \pm 1.1$  Kiss1-ir pixels/area; t-test,  $P = 0.94$ ). Similarly, there was no difference in total NKB fibres between control ( $9.45 \pm 2.2$  Kiss1-ir pixels/area) and lactating animals ( $10.67 \pm 1.52$  Kiss1-ir pixels/area; t-test,  $P = 0.66$ ). There was also no difference in the distribution of Kiss1 or NKB fibres or the percentage of colocalised fibres. Analysis of contact with GnRH fibres by Kiss1, NKB or Kiss1/NKB fibres could not be performed as a result of the extreme abundance of staining in the ME of both Kiss1 and NKB, as well as the transgenic labelling of GnRH.

Importantly, there was variability in NKB fibre staining within the ME, regardless of group, particularly with the quantity of single-labelled fibres in the external zone varying within individual cases. Two examples from the same animal are shown in Fig. 2, with one section containing conspicuous NKB-ir fibres in the external zone (Fig. 2A–D) and another section containing few NKB-ir fibres in the external zone (Fig. 2E–H). None of the variability between sections could be accounted for by rostral-caudal position.

To verify the results obtained by fluorescence secondary detection demonstrating section-to-section variability in the quantity of NKB fibres in the external zone of the ME, chromagen (NiDAB) detection was also performed. Although NiDAB detection cannot be used to detect colocalised Kiss1/NKB-ir fibres, it was possible to compare the distribution of NKB-ir fibres within the external zone of the ME to fluorescent detection. Similar to results obtained by fluorescence double-label immunohistochemistry, we observed variability in the quantity of NKB fibres in the external zone of the ME within individual cases by NiDAB labelling (Fig. 3). Once again, two examples from one animal are shown, with one section containing conspicuous fibres in the external zone (Fig. 3B,C) and other section containing quite scattered fibres in the external zone (Fig. 3D,E). This variability was not accounted for by the rostral–caudal position. Staining of the ARH with NiDAB labelling was also consistent with immunofluorescence labelling (Figs 1A and 3A).

## Experiment 2: Rostral projections of ARH Kiss1/NKB neurones

To characterise ARH Kiss1/NKB rostral fibre projections, as well as single Kiss1 and NKB fibre distributions, immunohistochemistry was performed and used to compile computer-assisted line drawings of these fibres. Immunohistochemistry revealed a primarily ventricular projection of ARH Kiss1/NKB-ir fibres (Fig. 4), as observed at the level of the anterior periventricular region (Figs 4D and 5A), and these double-labelled fibres were diminished in more rostral sections at the level of the AVPV (Figs 4B and 5B). Importantly, double-label fibres appeared to diminish significantly before the level of GnRH neurones in the NDB and few double-labelled Kiss1/NKB-ir fibres were observed at this level (Figs 4A and 5C,D). There were also very few double-labelled Kiss1/NKB-ir fibres near GnRH neurones in other areas of the POA (results not shown). Quantification of colocalisation in control animals using Manders' coefficient, revealed that only 2.6% ( $\pm 0.85$ ,  $n = 4$ ) of Kiss1 staining overlapped with NKB staining at the level of GnRH neurones in the medial septal nucleus and NDB (Fig. 5C), whereas 5.1% ( $\pm 0.82$ ,  $n = 4$ ) of NKB staining overlapped with Kiss1 staining. NKB colocalisation was likely slightly higher because of the smaller number of NKB fibres in this area. In summary, ARH Kiss1/NKB projections are found medially along the ventricle, and this appears to be the predominant rostral projection path of Kiss1/NKB fibres because very few Kiss1/NKB fibres were observed in lateral nuclei of the

hypothalamus (Fig. 4D–F), and they diminished significantly before the POA regions containing GnRH neurones.

Single-labelled Kiss1-ir and NKB-ir fibres were found along the ventricle as well as at the level of the GnRH neurones in the NDB and the broader POA (Fig. 5C,D). Particularly, single-labelled Kiss1-ir fibres were abundant near GnRH neurones, which is consistent with the known projections out of the AVPV, where there is an additional Kiss1 population in the rat. Single-labelled Kiss1 and NKB fibres were also found in many lateral hypothalamic areas (Fig. 4D–F).

To determine whether lactation resulted in any significant difference in total Kiss1-ir or NKB-ir staining, sections of the POA at the level of GnRH cell bodies were analysed for total Kiss-ir and NKB-ir staining, as measured by pixels. Surprisingly, total Kiss1-ir total staining appeared to be significantly increased in the lactating group compared to the control group. The total number of Kiss1-ir pixels in a size constant area of the POA was, on average,  $8150 \pm 1182$  pixels in the control group ( $n = 4$ ), whereas the average number of pixels for the lactating group ( $n = 3$ ) was  $19988 \pm 657$  pixels (t-test,  $P < 0.05$ ). By contrast, total NKB-ir pixels did not change in the POA between lactating ( $5981$  pixels  $\pm 1006$ ) and control groups ( $6300$  pixels  $\pm 539$ ; t-test  $P = 0.81$ ). To determine whether increased Kiss1-ir fibres in the POA translated to increased contacts with GnRH cell bodies, analysis of Kiss1-ir close appositions on GnRH cell bodies was performed. Ten cells were analysed per animal, from the same photomicrographs used to quantify of total Kiss1-ir in the POA. There was no significant difference in the number of Kiss1 single-labelled fibre appositions on GnRH neurones between control and lactating animals (t-test,  $P = 0.26$ ). Of the GnRH cells investigated,  $32.5 \pm 13\%$  had close appositions from single-labelled Kiss1 fibres, whereas  $40 \pm 5.8\%$  had close appositions from these fibres in lactating animals. Furthermore, these values of Kiss1 fibre close appositions on GnRH neurones are similar to those reported previously both in the sheep and mouse (25, 34). By contrast to single-labelled Kiss-1-ir close appositions, out of the 70 GnRH neurones studied, only two had close appositions from Kiss1/NKB double-labelled fibres.

### Experiment 3: Regulation of Kiss1 and NKB populations during lactation

**ARH Kiss1/NKB**—ARH Kiss1/NKB neurones were found to have projections in the ME near GnRH fibres, suggesting a potential regulatory relationship between these ARH peptides and GnRH release. This finding prompted the question of whether changes in ARH Kiss1/NKB during lactation may be responsible for decreased GnRH release. Previous data have demonstrated a decrease in *Kiss1* and *NKB* mRNA within the ARH during the negative energy balance model of lactation (18, 19), and immunohistochemistry was performed to determine whether Kiss1 and NKB peptides are also decreased. In the ARH, both Kiss1 and NKB NiDAB immunoreactive staining was decreased in lactating animals compared to intact dioestrous animals (Fig. 6A,B,D,E) consistent with previous findings (19). There was also a significant reduction in cell number in lactating animals versus controls for both neuropeptides (Fig. 6C,F).

**AVPV Kiss**—The AVPV Kiss1 population has also been implicated as a critical component of GnRH regulation, particularly positive oestrogen feedback. *Kiss1* mRNA and peptide were measured in the AVPV to determine what, if any, changes occur during lactation in this population. Immunohistochemistry revealed an increase in Kiss1-ir cell number during lactation (Fig. 7A–C). However, *in situ* hybridisation revealed a significant decrease in *Kiss1* mRNA in the AVPV during lactation (Fig. 7D–F). These findings could suggest an inhibition of AVPV Kiss1 production as well as peptide release leading to an accumulation of peptide within cell bodies. This accumulation may also account for the



apparent increase in total Kiss1-ir in the POA because peptide likely accumulated in fibres as well.

## Discussion

The singularity of GnRH release as a final reproductive output signal from the brain suggests that there is likely an integrated regulation of these cells by many upstream neuronal populations. In the present study, GnRH inhibition during lactation was found to be coincident with the inhibition of ARH Kiss1/NKB peptide levels, consistent with previous findings of inhibited Kiss1 and NKB mRNA (18, 19). Double-label immunohistochemistry was used to track projections of colocalised ARH Kiss1/NKB cells in relation to GnRH cell bodies and fibres. The present study provides the first neuroanatomical evidence indicating that the opposing roles of the two Kiss1 populations in regulating steroid feedback of GnRH correlates with different sites of GnRH regulation (11, 35). The AVPV Kiss1 population contributes to positive steroid feedback and this regulation takes place at the level of the POA where Kiss1 fibres, likely originating from the AVPV, contact GnRH neurones (25). The present study demonstrated that most ARH Kiss1/NKB axons do not target GnRH cell bodies but instead project to the ARH-ME area where GnRH fibres terminate. Because ARH Kiss1/NKB cells are linked to negative steroid feedback (10), this suggests that, although positive feedback occurs at the level of GnRH cell bodies, negative feedback occurs at the level of GnRH fibres in the ME.

Importantly, the present study has found that the majority of Kiss1 and NKB staining in the ME does not represent colocalised Kiss1/NKB fibres from the ARH, similar to a recent study in the monkey reporting both single-labelled Kiss1 and NKB fibres in the ME (15). One explanation is that nuclei other than the ARH send significant Kiss1 and NKB projections to the ME, and the possible sources of such single-labelled Kiss1 and NKB are discussed below. Another explanation is that the beaded nature of Kiss1 and NKB staining in the ME may hamper the detection of double-labelled fibres during analysis. Particularly, anecdotal cases can be seen when scanning through 0.5  $\mu\text{m}$  planes in which a beads-on-a-string type fibre can be seen where some beads appear single-labelled for either Kiss1 or NKB, whereas other beads appear colocalised. Thus, our current immunohistochemistry methods may be flawed and underestimate the percentage of colocalised fibres.

Immunohistochemistry identifying Kiss1/NKB fibres in the ME demonstrated some variability with either fluorescence or NiDAB detection. In particular, there appeared to be section-to-section variability in the quantity of NKB fibres in external zone of the ME within individual cases, and this variability did not appear to have a rostral-caudal pattern. Therefore, caution should be used when characterising NKB fibres in this area because different distribution patterns could be concluded based on sections taken from the same animal. Overall, labelling in the external ME revealed a moderate number of periportal axons, thus indicating that their modulatory influence is potent or, alternatively, that an abundant supply of axons in the external ME releases the neuropeptides at a high rate preventing their accumulation and subsequent visualisation. Interestingly, DAB detection of the Kiss1 antibody also revealed occasional Kiss1 fibres in the external zone (unpublished observations, current authors); thus, it is possible that external zone fibres contain both Kiss1 and NKB but that this was not detected with fluorescence labelling for some unknown technical reason. Another possibility could be that Kiss1 staining is also labelling RFRP-1 because, although we did not detect labelling in the DMH where RFRP-1 cell bodies reside, this does not exclude the possibility that RFRP-1 fibres could be labelled with the Kiss1 antibody. However, this appears unlikely because the distribution of Kiss1 fibres observed is similar to that seen by Desroziers *et al.* (32), including occasional Kiss1 fibres in the external zone of the ME, as well as a recent nonhuman primate study by Ramaswamy *et al.*

(15), which found colocalised Kiss1/NKB fibres predominantly in the internal zone. Improved antibodies will be needed to verify whether the few NKB or Kiss1 fibres reported to project into the external zone in the present study are ARH Kiss1/NKB projections.

The lack of significant Kiss1/NKB fibres in the external zone has been a confounding issue in determining whether the ME is truly a site of regulation because GnRH terminals are in the external zone. One possibility is that Kiss1/NKB fibres do extend into the external zone, although peptide release is so fast that peptide cannot be detected with immunohistochemistry. Another possibility is that Kiss1/NKB is released into the internal zone and travels by diffusion to the external zone to bind receptors on GnRH terminals. Importantly, the nonhuman primate does not show significant Kiss1 contacts at GnRH cell bodies but Kiss1 fibres are near GnRH fibres in the internal zone of the ME (15, 36). Despite this lack of contact at GnRH cell bodies, Kiss1 administration still causes robust release of GnRH in nonhuman primates (15, 37), suggesting that Kiss1 may regulate GnRH release directly from the ME through nonsynaptic regulation.

Unexpectedly, total Kiss1-ir and NKB-ir staining in the ME did not decrease in the lactating condition, despite decreases in both Kiss1-ir and NKB-ir in the ARH. This finding using fluorescence labelling was also confirmed qualitatively with DAB staining (results not shown), suggesting that there is likely inhibition of Kiss1 and NKB release in the ME and accumulation of the peptides within fibres. A similar phenomenon seemed to be occurring in the AVPV as well. Although AVPV *Kiss1* mRNA was decreased during lactation, peptide was increased at the level of cell bodies, and total Kiss1-ir fibre staining was increased at the level of the POA. The increase in Kiss1-ir in the POA during lactation did not translate to a higher percentage of GnRH neurones demonstrating close appositions from single-labelled Kiss1-ir fibres, supporting the hypothesis that higher peptide levels in the POA are associated with inhibition of release and not upregulation of synapses with GnRH neurones. Importantly, the data from the ME and POA suggest that inhibition of peptide release is a common mechanism in both Kiss1 populations, although it may be more severe in the AVPV population because total peptide was actually increased in both cells and fibres.

In addition to the ARH Kiss1/NKB fibre projections to the ME, there were also major rostral projections along the third ventricle. The ARH Kiss1/NKB fibres diminish significantly prior to GnRH neurones, so it is unclear what the function of these rostral projections may be. Many other cell populations rostral to the ARH are also involved in GnRH regulation and thus could be targets for direct regulation by ARH Kiss1/NKB. The orexin and MCH cell populations are prime candidates because GnRH neurones express the orexin and MCH receptors and both fibre types are known to contact GnRH cell bodies (38, 39). However, these cells are located in the lateral hypothalamus, whereas the predominant ARH Kiss1/NKB projections were found only medially along the ventricle; thus, it is unlikely that these cells are directly regulated by ARH Kiss1/NKB projections. Further research will be needed to determine what, if any, role these rostral ARH Kiss1/NKB play in GnRH regulation. In addition, the lack of Kiss1/NKB direct projections to GnRH cell bodies or terminals suggests that these neurones may likely be involved in more than just GnRH regulation but, to date, little research has focused on this topic.

The AVPV is likely the source of single-labelled Kiss1 fibres because this is the other predominant Kiss1 population in the rat. In agreement with this idea, the AVPV is known to regulate reproductive function via projections to GnRH cell bodies in the POA, and many studies have specifically identified the Kiss1 population of this nucleus as an important contributor to oestrogen-mediated positive feedback (2, 40, 41). However, Kiss1 input from the AVPV may also contribute to basal stimulation of GnRH neurones, such that a decrease

in AVPV Kiss1 drive onto GnRH cells during lactation may lead to downstream decreases in GnRH release.

The origins of the single-NKB fibres in the POA are less clear. By immunohistochemistry, the next most abundant population of NKB cells is in the BST and this nucleus has been previously implicated in reproductive regulation (42, 43). Initial studies indicated that, during lactation, there was an increase in NKB peptide in the BST, although no change in mRNA arguing against inhibition of this nucleus during lactation (results not shown). Although the BST is the next biggest cell population of NKB after the ARH, NKB peptide and mRNA have been localised to many areas of the brain including the cerebral cortex, amygdaloid complex and lateral mammillary bodies (26). It is possible that single-label NKB fibres in the NDB and POA arrive from one or many of these additional nuclei.

Overall, the finding of inhibited ARH Kiss1/NKB and AVPV Kiss1 populations during lactation is consistent with the hypothesis that decreased GnRH release in this model is a result of decreases in upstream stimulatory tone. However, the signals responsible for inhibition of Kiss1 during lactation remain largely unknown. Kiss1 has been shown to be inhibited in another model of negative energy balance (i.e. fasting) and the predominant hypothesis in this model is that low leptin drives Kiss1 and LH inhibition (44–48). However, previous work in the lactating model has demonstrated ARH Kiss1/NKB mRNA and serum LH levels remain low even after leptin is restored to physiological levels, suggesting that low leptin is not required for inhibition of ARH Kiss1/NKB in this model (18). This discrepancy between fasting and lactation may be due to obvious differences in the duration and severity of negative energy balance between the two models. It is also possible that leptin was incapable of restoring ARH Kiss1/NKB and LH levels during lactation as a result of another redundant inhibitory signal in this model: the suckling stimulus. The suckling of pups activates cells in a large number of brainstem nuclei that project to the ARH and removal of this stimulus results in a rapid restoration of GnRH and LH release (18, 49, 50). It is therefore possible that inhibition of ARH Kiss1/NKB is driven in part by brainstem nuclei activated by suckling stimulus in the lactation model.

Regulation of NKB during negative energy balance is less well understood, as is the nature of the effects of NKB on GnRH release. Although NKB clearly appears to be stimulatory for GnRH release in humans, there are contradictory reports for the effect of NKB on LH release in other species (12, 14, 17, 51–53). More recent evidence has demonstrated that, although NKB acutely stimulates LH in sheep and nonhuman primates, intermittent administration cannot maintain pulsatile LH, which could account for contrasting reports on the actions of NKB on GnRH release (15, 54). The data reported in the present study are consistent with a stimulatory effect of NKB for GnRH release because epeptide and mRNA levels are decreased in the ARH during lactation when GnRH release is low (18). The NKB receptor, NK3, has been recently identified on ARH Kiss1/NKB cells, which has led to the hypothesis that ARH NKB may work in an autoregulatory manner to stimulate ARH Kiss1 release; thus, decreases in NKB could lead to decreased Kiss1 release, resulting in a reduced stimulatory tone for GnRH release (17, 55).

Although ARH Kiss1/NKB neurones likely directly influence GnRH fibres in the ME and these ARH cells are inhibited during lactation, the question of whether inhibition of these nuclei is required for GnRH and LH inhibition in this model remains unanswered. It is also possible that Kiss1/NKB modulation of GnRH release is in part indirect via dopaminergic terminals in the external ME, in line with recent studies (56) showing an association of Kiss1 axons with the perikarya of dopaminergic tubero-infundibular neurones of the ARH. *In vitro* techniques such as hypothalamic explants may allow for a more direct approach to address whether Kiss1 and NKB peptide release is decreased in tissue from animals in

negative energy balance and what if any effect restoring these peptides has on GnRH release. Although the present study did not directly measure release of Kiss1 and NKB, it has provided evidence that the ARH Kiss1/NKB cells, and likely the AVPV Kiss1 cells as well, are inhibited during lactation when GnRH release is low. Importantly, the present study is the first to definitively demonstrate an absence of ARH Kiss1/NKB projections to GnRH neurones in the POA, and suggests that this population likely regulates GnRH activity via projections to the ARH-ME area.

## Acknowledgments

We gratefully acknowledge our funding source (HD14643, RR00163), as well as the Oregon National Primate Research Center Endocrine Assay Core and the University of Virginia Center for Research in reproduction Ligand Assay and Analysis Core supported by the Eunice Kennedy Shriver NICHD/NIH (SCCPIR) Grant U54-HD28934.

## References

- Gottsch ML, Clifton DK, Steiner RA. Kisspeptin-GPR54 signaling in the neuroendocrine reproductive axis. *Mol Cell Endocrinol.* 2006; 254–255:91–96.
- Popa SM, Clifton DK, Steiner RA. The role of kisspeptins and GPR54 in the neuroendocrine regulation of reproduction. *Annu Rev Physiol.* 2008; 70:213–238. [PubMed: 17988212]
- Roa J, Aguilar E, Dieguez C, Pinilla L, Tena-Sempere M. New frontiers in kisspeptin/GPR54 physiology as fundamental gatekeepers of reproductive function. *Front Neuroendocrinol.* 2008; 29:48–69. [PubMed: 17870152]
- Smith JT, Clifton DK, Steiner RA. Regulation of the neuroendocrine reproductive axis by kisspeptin-GPR54 signaling. *Reproduction.* 2006a; 131:623–630. [PubMed: 16595713]
- de Roux N, Genin E, Carel JC, Matsuda F, Chaussain JL, Milgrom E. Hypogonadotropic hypogonadism due to loss of function of the KiSS1-derived peptide receptor GPR54. *Proc Natl Acad Sci USA.* 2003; 100:10972–10976. [PubMed: 12944565]
- Seminara SB, Messager S, Chatzidaki EE, Thresher RR, Acierno JS Jr, Shagoury JK, Bo-Abbas Y, Kuohung W, Schwinof KM, Hendrick AG, Zahn D, Dixon J, Kaiser UB, Slaugenhaupt SA, Gusella JF, O’Rahilly S, Carlton MB, Crowley WF Jr, Aparicio SA, Colledge WH. The GPR54 gene as a regulator of puberty. *N Engl J Med.* 2003; 349:1614–1627. [PubMed: 14573733]
- Matsui H, Takatsu Y, Kumano S, Matsumoto H, Ohtaki T. Peripheral administration of metastatin induces marked gonadotropin release and ovulation in the rat. *Biochem Biophys Res Commun.* 2004; 320:383–388. [PubMed: 15219839]
- Navarro VM, Castellano JM, Fernandez-Fernandez R, Barreiro ML, Roa J, Sanchez-Criado JE, Aguilar E, Dieguez C, Pinilla L, Tena-Sempere M. Developmental and hormonally regulated messenger ribonucleic acid expression of KiSS-1 and its putative receptor, GPR54, in rat hypothalamus and potent luteinizing hormone-releasing activity of KiSS-1 peptide. *Endocrinology.* 2004; 145:4565–4574. [PubMed: 15242985]
- Navarro VM, Castellano JM, Fernandez-Fernandez R, Tovar S, Roa J, Mayen A, Barreiro ML, Casanueva FF, Aguilar E, Dieguez C, Pinilla L, Tena-Sempere M. Effects of KiSS-1 peptide, the natural ligand of GPR54, on follicle-stimulating hormone secretion in the rat. *Endocrinology.* 2005; 146:1689–1697. [PubMed: 15637288]
- Smith JT, Cunningham MJ, Rissman EF, Clifton DK, Steiner RA. Regulation of Kiss1 gene expression in the brain of the female mouse. *Endocrinology.* 2005; 146:3686–3692. [PubMed: 15919741]
- Uenoyama Y, Tsukamura H, Maeda KI. Kisspeptin/metastatin: a key molecule controlling two modes of gonadotrophin-releasing hormone/luteinising hormone release in female rats. *J Neuroendocrinol.* 2009; 21:299–304. [PubMed: 19210293]
- Topaloglu AK, Reimann F, Guclu M, Yalin AS, Kotan LD, Porter KM, Serin A, Mungan NO, Cook JR, Ozbek MN, Imamoglu S, Akalin NS, Yuksel B, O’Rahilly S, Semple RK. TAC3 and TACR3 mutations in familial hypogonadotropic hypogonadism reveal a key role for Neurokinin B in the central control of reproduction. *Nat Genet.* 2009; 41:354–358. [PubMed: 19079066]

13. Rance NE. Menopause and the human hypothalamus: evidence for the role of kisspeptin/neurokinin B neurons in the regulation of estrogen negative feedback. *Peptides*. 2009; 30:111–122. [PubMed: 18614256]
14. Rance NE, Young WS 3rd. Hypertrophy and increased gene expression of neurons containing neurokinin-B and substance-P messenger ribonucleic acids in the hypothalami of postmenopausal women. *Endocrinology*. 1991; 128:2239–2247. [PubMed: 1708331]
15. Ramaswamy S, Seminara SB, Ali B, Ciofi P, Amin NA, Plant TM. Neurokinin B stimulates GnRH release in the male monkey (*Macaca mulatta*) and is colocalized with Kisspeptin in the arcuate nucleus. *Endocrinology*. 2010; 151:4494–4503. [PubMed: 20573725]
16. Goodman RL, Lehman MN, Smith JT, Coolen LM, de Oliveira CV, Jafarzadehshirazi MR, Pereira A, Iqbal J, Caraty A, Ciofi P, Clarke IJ. Kisspeptin neurons in the arcuate nucleus of the ewe express both dynorphin A and neurokinin B. *Endocrinology*. 2007; 148:5752–5760. [PubMed: 17823266]
17. Navarro VM, Gottsch ML, Chavkin C, Okamura H, Clifton DK, Steiner RA. Regulation of gonadotropin-releasing hormone secretion by kisspeptin/dynorphin/neurokinin B neurons in the arcuate nucleus of the mouse. *J Neurosci*. 2009; 29:11859–11866. [PubMed: 19776272]
18. Xu J, Kirigiti MA, Grove KL, Smith MS. Regulation of food intake and gonadotropin-releasing hormone/luteinizing hormone during lactation: role of insulin and leptin. *Endocrinology*. 2009; 150:4231–4240. [PubMed: 19470705]
19. Yamada S, Uenoyama Y, Kinoshita M, Iwata K, Takase K, Matsui H, Adachi S, Inoue K, Maeda KI, Tsukamura H. Inhibition of metastin (kisspeptin- 54)-GPR54 signaling in the arcuate nucleus-median eminence region during lactation in rats. *Endocrinology*. 2007; 148:2226–2232. [PubMed: 17289848]
20. Clarkson J, d'Anglemont de Tassigny X, Moreno AS, Colledge WH, Herbison AE. Kisspeptin-GPR54 signaling is essential for preovulatory gonadotropin-releasing hormone neuron activation and the luteinizing hormone surge. *J Neurosci*. 2008; 28:8691–8697. [PubMed: 18753370]
21. Herbison AE. Estrogen positive feedback to gonadotropin-releasing hormone (GnRH) neurons in the rodent: the case for the rostral periventricular area of the third ventricle (RP3V). *Brain Res Rev*. 2008; 57:277–287. [PubMed: 17604108]
22. Irwig MS, Fraley GS, Smith JT, Acohido BV, Popa SM. Kisspeptin activation of gonadotropin releasing hormone neurons and regulation of KiSS- 1 mRNA in the male rat. *Neuroendocrinology*. 2005; 80:264–272. [PubMed: 15665556]
23. Krajewski SJ, Anderson MJ, Iles-Shih L, Chen KJ, Urbanski HF, Rance NE. Morphologic evidence that neurokinin B modulates gonadotropin-releasing hormone secretion via neurokinin 3 receptors in the rat median eminence. *J Comp Neurol*. 2005; 489:372–386. [PubMed: 16025449]
24. Quaynor S, Hu L, Leung PK, Feng H, Mores N, Krsmanovic LZ, Catt KJ. Expression of a functional g protein-coupled receptor 54-kisspeptin autoregulatory system in hypothalamic gonadotropin-releasing hormone neurons. *Mol Endocrinol*. 2007; 21:3062–3070. [PubMed: 17698953]
25. Clarkson J, Herbison AE. Postnatal development of kisspeptin neurons in mouse hypothalamus; sexual dimorphism and projections to gonadotropin-releasing hormone neurons. *Endocrinology*. 2006; 147:5817–5825. [PubMed: 16959837]
26. Marksteiner J, Sperk G, Krause JE. Distribution of neurons expressing neurokinin B in the rat brain: immunohistochemistry and *in situ* hybridization. *J Comp Neurol*. 1992; 317:341–356. [PubMed: 1374442]
27. Franceschini I, Lomet D, Cateau M, Delsol G, Tillet Y, Caraty A. Kisspeptin immunoreactive cells of the ovine preoptic area and arcuate nucleus co-express estrogen receptor alpha. *Neurosci Lett*. 2006; 401:225–230. [PubMed: 16621281]
28. Ciofi P, Krause JE, Prins GS, Mazzuca M. Presence of nuclear androgen receptor-like immunoreactivity in neurokinin B-containing neurons of the hypothalamic arcuate nucleus of the adult male rat. *Neurosci Lett*. 1994; 182:193–196. [PubMed: 7715808]
29. Bolte S, Cordelieres FP. A guided tour into subcellular colocalization analysis in light microscopy. *J Microsc*. 2006; 224:213–232. [PubMed: 17210054]

30. Gottsch ML, Cunningham MJ, Smith JT, Popa SM, Acohido BV, Crowley WF, Seminara S, Clifton DK, Steiner RA. A role for kisspeptins in the regulation of gonadotropin secretion in the mouse. *Endocrinology*. 2004; 145:4073–4077. [PubMed: 15217982]
31. Brailoiu GC, Dun SL, Ohsawa M, Yin D, Yang J, Chang JK, Brailoiu E, Dun NJ. KiSS-1 expression and metastin-like immunoreactivity in the rat brain. *J Comp Neurol*. 2005; 481(3):314–329. [PubMed: 15593369]
32. Desroziers E, Mikkelsen J, Simonneaux V, Keller M, Tillet Y, Caraty A, Franceschini I. Mapping of kisspeptin fibres in the brain of the prooestrus rat. *J Neuroendocrinol*. 2010; 22:1101–1112. [PubMed: 20673302]
33. Krajewski SJ, Burke MC, Anderson MJ, McMullen NT, Rance NE. Forebrain projections of arcuate neurokinin B neurons demonstrated by anterograde tract-tracing and monosodium glutamate lesions in the rat. *Neuroscience*. 2009; 166:680–697. [PubMed: 20038444]
34. Smith JT, Coolen LM, Kriegsfeld LJ, Sari IP, Jaafarzadehshirazi MR, Maltby M, Bateman K, Goodman RL, Tilbrook AJ, Ubuka T, Bentley GE, Clarke IJ, Lehman MN. Variation in kisspeptin and RFamide-related peptide (RFRP) expression and terminal connections to gonadotropin-releasing hormone neurons in the brain: a novel medium for seasonal breeding in the sheep. *Endocrinology*. 2008; 149:5770–5782. [PubMed: 18617612]
35. Oakley AE, Clifton DK, Steiner RA. Kisspeptin signaling in the brain. *Endocr Rev*. 2009; 30:713–743. [PubMed: 19770291]
36. Ramaswamy S, Guerriero KA, Gibbs RB, Plant TM. Structural interactions between kisspeptin and GnRH neurons in the mediobasal hypothalamus of the male rhesus monkey (*Macaca mulatta*) as revealed by double immunofluorescence and confocal microscopy. *Endocrinology*. 2008; 149:4387–4395. [PubMed: 18511511]
37. Ramaswamy S, Seminara SB, Pohl CR, DiPietro MJ, Crowley WF Jr, Plant TM. Effect of continuous intravenous administration of human metastin 45–54 on the neuroendocrine activity of the hypothalamic-pituitary-testicular axis in the adult male rhesus monkey (*Macaca mulatta*). *Endocrinology*. 2007; 148:3364–3370. [PubMed: 17412800]
38. Campbell RE, Grove KL, Smith MS. Gonadotropin-releasing hormone neurons coexpress orexin 1 receptor immunoreactivity and receive direct contacts by orexin fibers. *Endocrinology*. 2003; 144:1542–1548. [PubMed: 12639939]
39. Williamson-Hughes PS, Grove KL, Smith MS. Melanin concentrating hormone (MCH): a novel neural pathway for regulation of GnRH neurons. *Brain Res*. 2005; 1041:117–124. [PubMed: 15829220]
40. Dungan HM, Clifton DK, Steiner RA. Minireview: kisspeptin neurons as central processors in the regulation of gonadotropin-releasing hormone secretion. *Endocrinology*. 2006; 147:1154–1158. [PubMed: 16373418]
41. Smith JT, Popa SM, Clifton DK, Hoffman GE, Steiner RA. Kiss1 neurons in the forebrain as central processors for generating the preovulatory luteinizing hormone surge. *J Neurosci*. 2006b; 26:6687–6694. [PubMed: 16793876]
42. Polston EK, Gu G, Simerly RB. Neurons in the principal nucleus of the bed nuclei of the stria terminalis provide a sexually dimorphic GABAergic input to the anteroventral periventricular nucleus of the hypothalamus. *Neuroscience*. 2004; 123:793–803. [PubMed: 14706792]
43. Simerly RB, Chang C, Muramatsu M, Swanson LW. Distribution of androgen and estrogen receptor mRNA-containing cells in the rat brain: an *in situ* hybridization study. *J Comp Neurol*. 1990; 294:76–95. [PubMed: 2324335]
44. Castellano JM, Navarro VM, Fernandez-Fernandez R, Nogueiras R, Tovar S, Roa J, Vazquez MJ, Vigo E, Casanueva FF, Aguilar E, Pinilla L, Dieguez C, Tena-Sempere M. Changes in hypothalamic KiSS-1 system and restoration of pubertal activation of the reproductive axis by kisspeptin in undernutrition. *Endocrinology*. 2005; 146:3917–3925. [PubMed: 15932928]
45. Kalamatianos T, Grimshaw SE, Poorun R, Hahn JD, Coen CW. Fasting reduces KiSS-1 expression in the anteroventral periventricular nucleus (AVPV): effects of fasting on the expression of KiSS-1 and neuropeptide Y in the AVPV or arcuate nucleus of female rats. *J Neuroendocrinol*. 2008; 20:1089–1097. [PubMed: 18573184]

46. Kalra SP, Xu B, Dube MG, Moldawer LL, Martin D, Kalra PS. Leptin and ciliary neurotropic factor (CNTF) inhibit fasting-induced suppression of luteinizing hormone release in rats: role of neuropeptide Y. *Neurosci Lett*. 1998; 240:45–49. [PubMed: 9488171]
47. Luque RM, Kineman RD, Tena-Sempere M. Regulation of hypothalamic expression of KiSS-1 and GPR54 genes by metabolic factors: analyses using mouse models and a cell line. *Endocrinology*. 2007; 148:4601–4611. [PubMed: 17595226]
48. Nagatani S, Guthikonda P, Thompson RC, Tsukamura H, Maeda KI, Foster DL. Evidence for GnRH regulation by leptin: leptin administration prevents reduced pulsatile LH secretion during fasting. *Neuroendocrinology*. 1998; 67:370–376. [PubMed: 9662716]
49. Li C, Chen P, Smith MS. Identification of neuronal input to the arcuate nucleus (ARH) activated during lactation: implications in the activation of neuropeptide Y neurons. *Brain Res*. 1999a; 824:267–276. [PubMed: 10196458]
50. Li C, Chen P, Smith MS. Neural populations in the rat forebrain and brainstem activated by the suckling stimulus as demonstrated by cFos expression. *Neuroscience*. 1999b; 94:117–129. [PubMed: 10613502]
51. Corander MP, Challis BG, Thompson EL, Jovanovic Z, Loraine Tung YC, Rimmington D, Huhtaniemi IT, Murphy KG, Topaloglu AK, Yeo GS, O’Rahilly S, Dhillon WS, Semple RK, Coll AP. The effects of neurokinin B upon gonadotrophin release in male rodents. *J Neuroendocrinol*. 2010; 22:181–187. [PubMed: 20041982]
52. Kalra PS, Sahu A, Bonavera JJ, Kalra SP. Diverse effects of tachykinins on luteinizing hormone release in male rats: mechanism of action. *Endocrinology*. 1992; 131:1195–1201. [PubMed: 1380435]
53. Sandoval-Guzman T, Rance NE. Central injection of senktide, an NK3 receptor agonist, or neuropeptide Y inhibits LH secretion and induces different patterns of Fos expression in the rat hypothalamus. *Brain Res*. 2004; 1026:307–312. [PubMed: 15488494]
54. Billings HJ, Connors JM, Altman SN, Hileman SM, Holaskova I, Lehman MN, McManus CJ, Nestor CC, Jacobs BH, Goodman RL. Neurokinin B acts via the neurokinin-3 receptor in the retrochiasmatic area to stimulate luteinizing hormone secretion in sheep. *Endocrinology*. 2010; 151:3836–3846. [PubMed: 20519368]
55. Wakabayashi Y, Nakada T, Murata K, Ohkura S, Mogi K, Navarro VM, Clifton DK, Mori Y, Tsukamura H, Maeda K, Steiner RA, Okamura H. Neurokinin B and dynorphin A in kisspeptin neurons of the arcuate nucleus participate in generation of periodic oscillation of neural activity driving pulsatile gonadotropin-releasing hormone secretion in the goat. *J Neurosci*. 2010; 30:3124–3132. [PubMed: 20181609]
56. Szawka RE, Ribeiro AB, Leite CM, Helena CV, Franci CR, Anderson GM, Hoffman GE, Anselmo-Franci JA. Kisspeptin regulates prolactin release through hypothalamic dopaminergic neurons. *Endocrinology*. 2010; 151:3247–3257. [PubMed: 20410200]

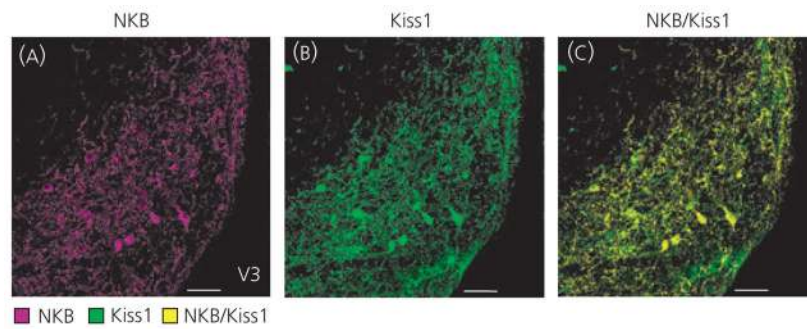


**Fig. 1.** Colocalisation of kisspeptin (Kiss1) and neurokinin B (NKB) in the arcuate nucleus (ARH). Immunohistochemical results of NKB-immunoreactive (ir) (A; magenta) and Kiss1-ir (B; green) staining in the ARH revealed almost complete colocalisation (C; yellow) of Kiss1 and NKB cell bodies within ovarioectomised virgin rats. Scale bars = 50  $\mu$ m; V3, third ventricle.



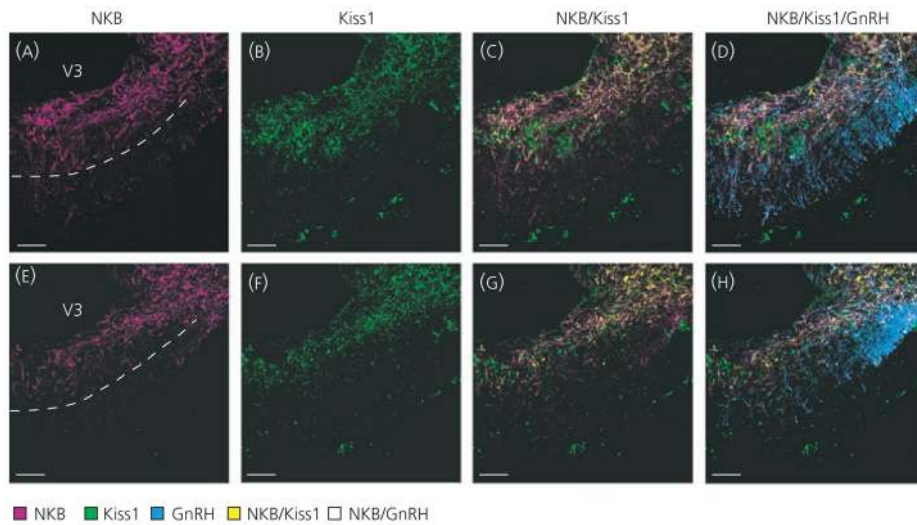


**Fig. 2.** Kisspeptin (Kiss1) and neurokinin B (NKB) fibre distribution in the median eminence (ME). NKB-immunoreactive (-ir) (A, E; magenta) and Kiss1-ir (B, F; green) fibres were found in the ME and overlay of these images revealed colocalised Kiss1/NKB-ir fibres (C, G; yellow) primarily in the internal zone. Doublelabelled Kiss1/NKB-ir fibres were observed in close proximity to gonadotrophin-releasing hormone-green fluorescent protein (GnRH-GFP) fibres (D, H; blue). Single-labelled Kiss1-ir fibres were also observed primarily in the internal zone, whereas single-labelled NKB-ir fibres were observed in both the internal and external zone of the ME. Single-labelled NKB-ir fibres were often found in close proximity to GnRH fibres in the external zone of the ME (white). Two ME examples from the same animal are shown to illustrate variability of staining within the external zone. The dotted lines in (A) and (E) mark the approximate border of the internal and external zone. Immunohistochemistry was performed in ovariectomised GnRH-GFP virgin rats. Scale bars = 50  $\mu$ m; V3, third ventricle.

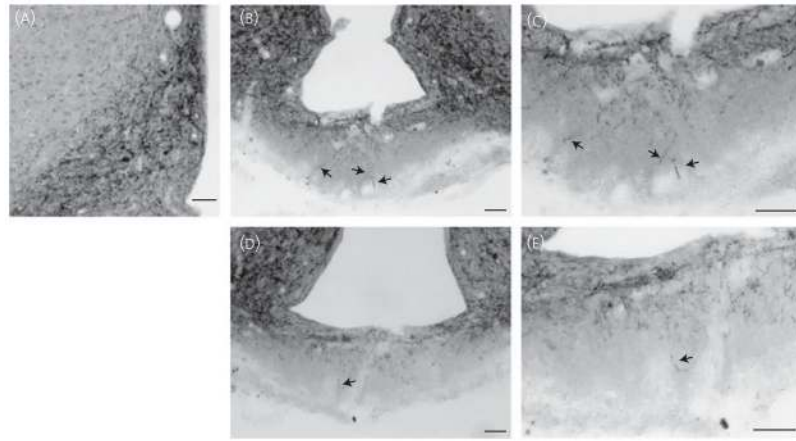


**Fig. 3.** Neurokinin B (NKB) immunoreactivity in the arcuate nucleus (ARH) and median eminence (ME) using nickel-intensified 3,3'-diaminobenzidine tetrahydrochloride (NiDAB) secondary detection. NiDAB staining was used to verify the variable quantity of NKB fibres in the external zone of the ME as observed by fluorescence labelling. ARH NKB-immuoreactivity (ir) (A) appeared similar to fluorescence immunoreactivity. The quantity of NKB-ir fibres in the external zone of the ME (arrows) varied from moderate (B, C) to light (D, E) in sections taken from the same ovariectomised virgin rat. (C, E) Magnifications of (B) and (D), respectively. Scale bars = 50  $\mu$ m.

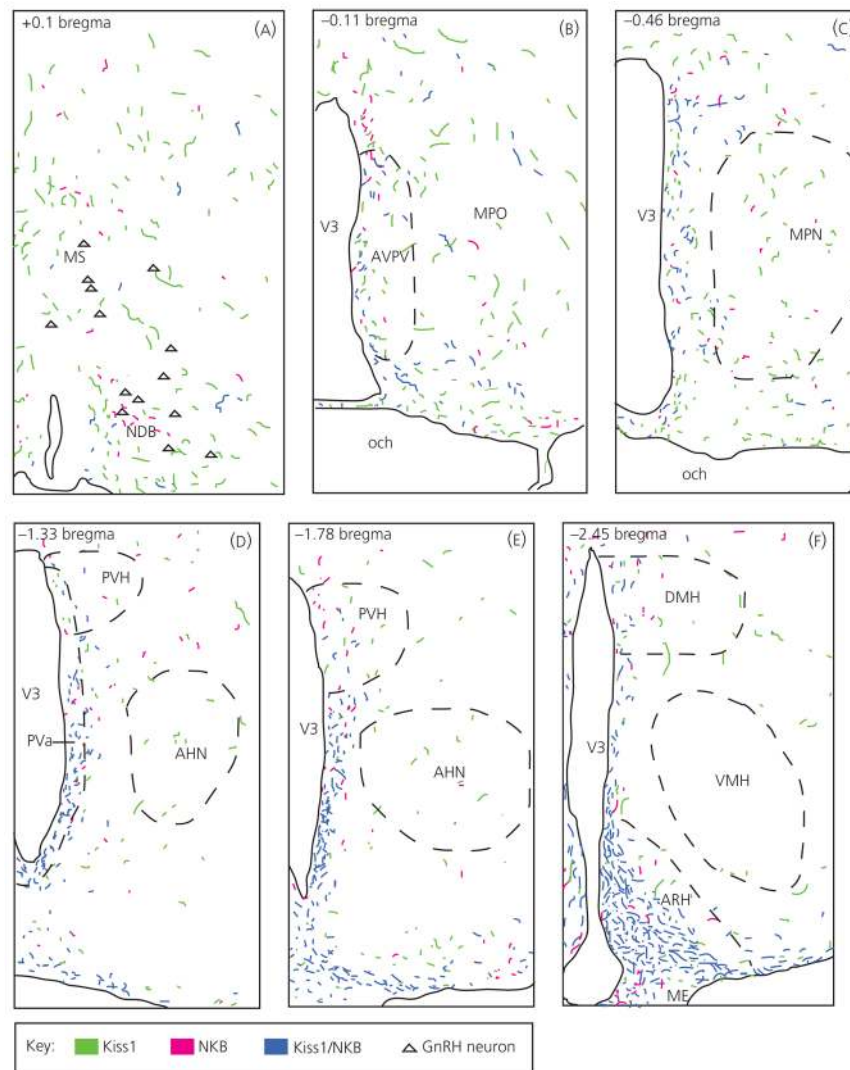


**Fig. 4.**

Computer assisted line drawings of kisspeptin (Kiss1)/neurokinin B (NKB)-immunoreactive (ir) rostral fibre projections from the arcuate nucleus. Double-labelled Kiss1/NKB-ir fibres (blue) in ovariectomised virgin control tissue had a rostral projection pattern that closely followed the third ventricle (V3) with fibres diminishing rostrally (panels A–F represent a rostral to caudal progression, beginning at the level of the NDB in panel A and ending at the level of the ARH in panel F). Very few double-labelled Kiss1/NKB-ir fibres were observed near gonadotrophin-releasing hormone (GnRH) neurones (A; triangles) in the NDB, although single-labelled Kiss1-ir fibres (green) and NKB-ir fibres (magenta) were found in this area. Corresponding coordinates from the Swanson rat brain atlas (30) are given in upper left corner of each panel. AHN, anterior hypothalamic nucleus; AVPV, anteroventral periventricular nucleus; DMH, dorsomedial nucleus of the hypothalamus; ME, median eminence; MPN, medial preoptic nucleus; MPO, medial preoptic area; MS, medial septal nucleus; NDB, nucleus of the diagonal band of Broca; och, optic chiasm; VMH, ventromedial nucleus hypothalamus.

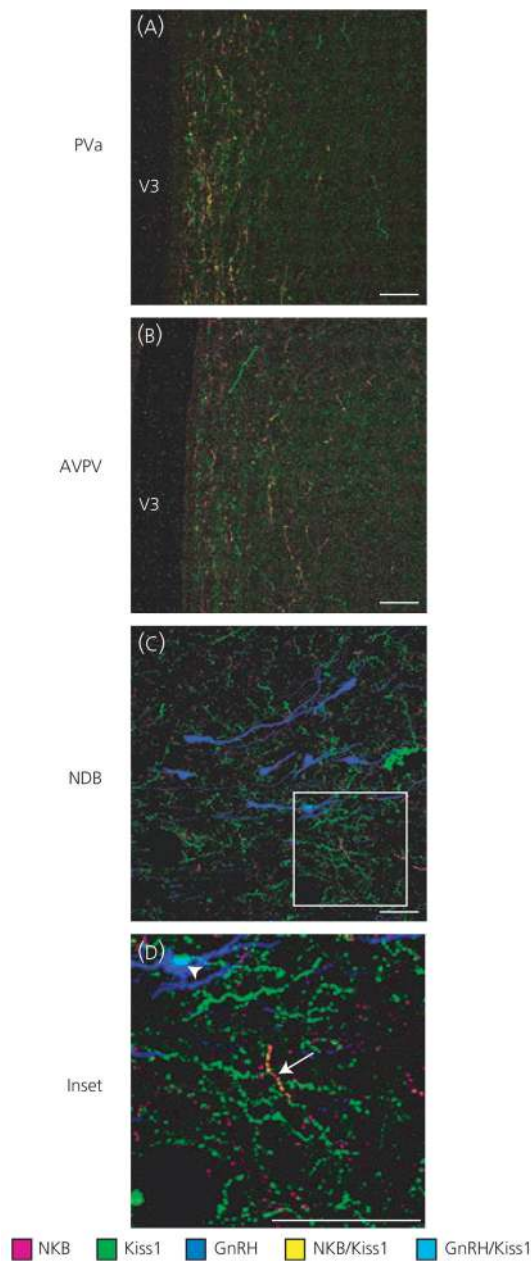


**Fig. 5.** Colocalised kisspeptin (Kiss1)/neurokinin B (NKB)-immunoreactive (ir) fibres at the level of the anterior periventricular nucleus (Pva), anteroventral periventricular nucleus (AVPV) and nucleus of the diagonal band of Broca (NDB). Double-label immunohistochemistry in gonadotrophin-releasing hormone-green fluorescent protein ovariectomised virgin control rats revealed a ventricular projection pattern of double-labelled Kiss1/NKB-ir fibres (A; yellow), which diminished rostrally (B), with few double-labelled fibres (C, D; arrow) observed in the NDB near GnRH neurones (blue). Single-labelled Kiss1-ir (green) and NKB-ir fibres (magenta) were observed at all three levels, with single-labelled Kiss1-ir fibres being particularly abundant in the NDB and some close contacts to GnRH neurones were observed (D; light blue, arrowhead). The coordinates of the three micrographs

correspond to the following panels in Fig. 4: (A) to Fig. 4(D), (B) to Fig. 4(B) and (C) to Fig. 4(A). Scale bars = 50  $\mu\text{m}$ .

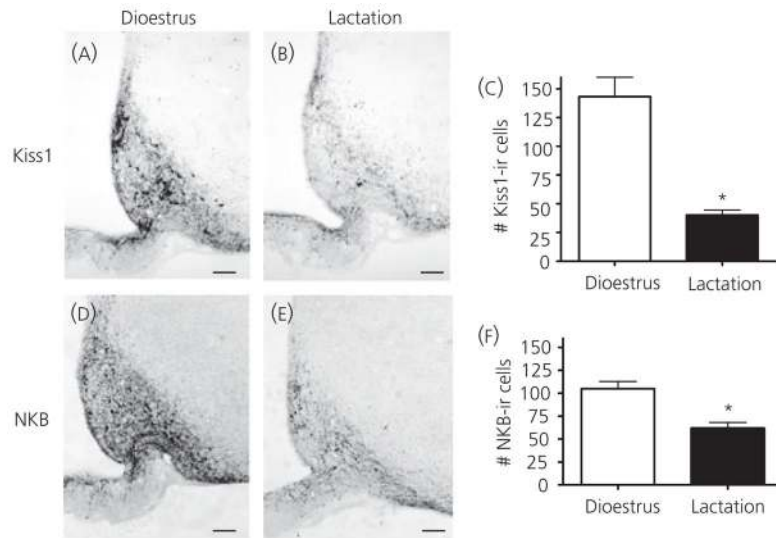


**Fig. 6.** Arcuate nucleus (ARH) kisspeptin (Kiss1) and neurokinin B (NKB) immunohistochemistry during dioestrus and lactation. Immunohistochemistry for Kiss1 (A, B) and NKB (D, E) revealed decreases in ARH Kiss1-immunoreactive (ir) positive cells in lactating animals ( $n = 4$ ) compared to dioestrus virgin controls ( $n = 4$ , E). ARH NKB-ir positive cell bodies were also decreased in intact lactating animals ( $n = 4$ ) compared to dioestrus virgin controls ( $n = 3$ , F). Cell numbers were counted as the total number of cells observed in four sections per animal. Scale bars =  $50 \mu\text{m}$ ; \* $P < 0.05$ .

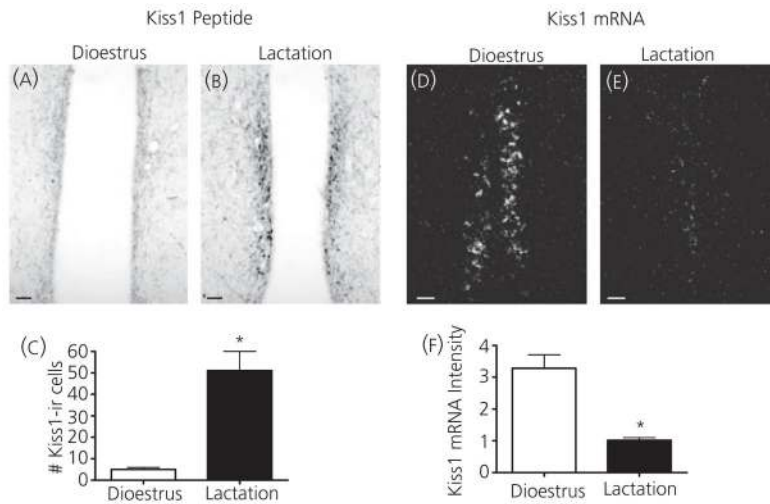


**Fig. 7.** Kisspeptin (Kiss1) peptide and mRNA in the anteroventral periventricular (AVPV) during dioestrus and lactation. The number of Kiss1-immunoreactive (ir) cells increased in the AVPV in intact lactating animals ( $n = 3$ ) compared to dioestrus virgin controls ( $n = 4$ ; A–C). Cell numbers were counted as the total number of cells observed in three sections per animal. *Kiss1* mRNA (D, E) significantly decreased in the AVPV in lactating animals ( $n = 6$ ) compared to dioestrus virgin controls ( $n = 5$ ) as measured by the averaged integrated intensity of silver grains using *in situ* hybridization (F). Scale bars = 50  $\mu\text{m}$ ; \* $P < 0.05$ .